# Human Glycinamide Ribonucleotide Transformylase: Active Site Mutants as Mechanistic Probes†

Wanda Manieri,‡ Molly E. Moore,‡,§ Matthew B. Soellner,‡,|| Pearl Tsang,⊥ and Carol A. Caperelli*,‡

*Division of Pharmaceutical Sciences, College of Pharmacy, University of Cincinnati Medical Center, P.O. Box 670004, Cincinnati, Ohio 45267, and Department of Chemistry, University of Cincinnati, P.O. Box 210172, Cincinnati, Ohio 45221*

*Received September 16, 2006; Revised Manuscript Received October 30, 2006*

ABSTRACT: Human glycinamide ribonucleotide transformylase (GART) (EC 2.1.2.2) is a validated target for cancer chemotherapy, but mechanistic studies of this therapeutically important enzyme are limited. Site-directed mutagenesis, initial velocity studies, pH−rate studies, and substrate binding studies have been employed to probe the role of the strictly conserved active site residues, N106, H108, and D144, and the semiconserved K170 in substrate binding and catalysis. Only two conservative substitutions, N106Q and K170R, resulted in catalytically active enzymes, and these active mutant enzymes gave pH−rate profiles and a steady-state kinetic mechanism essentially identical to those of the native enzyme. All inactive mutants were able to bind both substrates, ruling out disrupted formation of the ternary complex as the source of inactivity. Differences between human and *Escherichia coli* GART, previously used as a model for the human enzyme, were evident.

Glycinamide ribonucleotide transformylase (GART,[1] EC 2.1.2.2) catalyzes the transfer of the formyl group from $N^{10}$-formyltetrahydrofolate to the primary, side-chain amino group of glycinamide ribonucleotide (GAR) to yield formylglycinamide ribonucleotide (FGAR) and tetrahydrofolate (Scheme 1), ultimately resulting in the incorporation of C-8 into inosinic acid (IMP). This reaction is the third step and the first of two folate-dependent formyl transfers in the de novo purine biosynthetic pathway. GART was first discovered and partially characterized from pigeon liver in pioneering investigations by Warren and Buchanan (*1*).

The critical role that purine nucleotides play as precursors to RNA and DNA led to the suggestion that inhibition of de novo purine biosynthesis might be a viable approach toward cancer chemotherapy (*2*−*4*). This suggestion was confirmed when it was demonstrated that 5,10-dideazatetrahydrofolate, a potent antitumor agent, has, as its mechanism of action, the inhibition of GART and, consequently, of de novo purine biosynthesis (*5*).

This discovery led to a resurgence of interest in the de novo purine biosynthetic pathway and served as the impetus for numerous studies on the mechanism (*6*−*9*), structure (*10*−*15*), and structure-based design of inhibitors (*16*−*22*) for *Escherichia coli* GART, as a model for the human enzyme. *E. coli* GART was proposed as a model for the human enzyme because they share a high degree of homology and are mechanistically similar. An advantage of the *E. coli* enzyme is that it is a small (23 kDa) monofunctional, monomeric protein (*23*, *24*). In contrast, human GART comprises the C-terminal domain of a large (108 kDa), trifunctional enzyme that also catalyzes the synthesis of GAR (GARS) and the synthesis of aminoimidazole ribonucleotide (AIRS) (*25*, *26*). These additional activities catalyze steps 2 and 5 of the pathway.

The *E. coli* studies have provided useful information, including the identification of the wholly conserved residues, N106, H108, and D144, as catalytically important. However, more recent structure (*27*, *28*) and inhibition (*29*−*37*) studies have revealed differences between *E. coli* and human GART, and these results argue that the human enzyme represents the most relevant subject for further investigation. This is entirely feasible because the human GART domain has been cloned, overexpressed, and purified to homogeneity (*38*, *39*).

To date, few mechanistic or structural studies have been reported for human GART. These include the structures of the apo and ternary complex of rhGART (*28*), the structures of rhGART at low (pH 4.2) and high (pH 8.5) pH and in a binary complex with substrate $\beta$-GAR (*27*), nucleotide substrate specificity studies (*40*), structure-based inhibitor design and evaluation (*29*−*37*), and limited site-directed mutagenesis (*38*) of two of the wholly conserved residues (H108 and D144) implicated in the catalytic mechanism of the *E. coli* and human enzyme. The most recent inhibitor studies reinforce the conclusion that there are significant differences between *E. coli* and human GART.

In this report we describe more extensive site-directed mutagenesis of selected conserved residues, N106, H108,

† Supported by NIH Grant GM61194.

* To whom correspondence should be addressed: e-mail, Carol.Caperelli@uc.edu; phone, (513) 558-0730; fax, (513) 558-0978.

‡ College of Pharmacy, University of Cincinnati Medical Center.

§ WISE-REU participant, summer 2004.

|| Current address: Department of Chemistry, University of California—Berkeley, Berkeley, CA.

⊥ Department of Chemistry, University of Cincinnati.

[1] Abbreviations: GART, glycinamide ribonucleotide transformylase; GAR, glycinamide ribonucleotide; FGAR, formylglycinamide ribonucleotide; GARS, glycinamide ribonucleotide synthetase; AIRS, aminoimidazole ribonucleotide synthetase; rhGART, recombinant human glycinamide ribonucleotide transformylase; fDDF, 10-formyl-5,8-dideazafolate; aDDF, 10-acetyl-5,8-dideazafolate; GAR-OH, hydroxyacetamide ribonucleotide.

10.1021/bi0619270 CCC: $37.00 
Published on Web 01/02/2007

Scheme 1

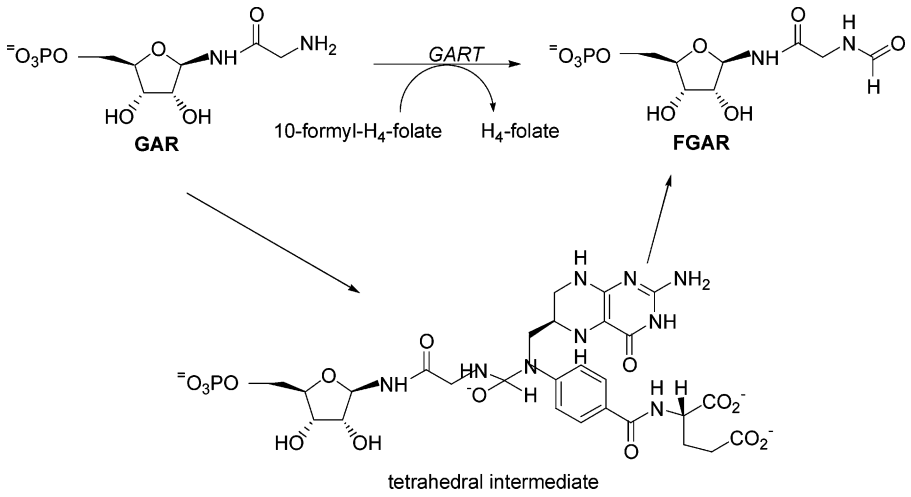


and D144, as well as K170, kinetic and substrate binding data for the mutant proteins, and pH−rate data for the catalytically active mutants. This constitutes the first mechanistic characterization of catalytic mutants of human GART.

## MATERIALS AND METHODS

*Materials.* Desalted synthetic oligonucleotides were obtained from IDT, Inc. Restriction enzymes were purchased from New England Biolabs, Promega, and Fermentas, T4 DNA ligase was from New England Biolabs, and DNase was from Fermentas. pMAL-c2x and pET17b were purchased from New England Biolabs and Novagen, respectively. The QuikChange kit from Stratagene was used for site-directed mutagenesis. Rosetta(DE3) cells were from Novagen, BL21Star(DE3) cells were from Invitrogen, and chemically competent DH5α cells were from Protein Express (Cincinnati, OH). The Wizard SV gel and PCR clean-up system was obtained from Promega. Perfect Prep plasmid mini and midi kits and the TripleMaster PCR system were from Eppendorf. QAE-Sephadex A-25, ovomucoid, SBTI, aprotinin, pepstatin, leupeptin, benzamidine, PMSF, DTT, and lysozyme were purchased from Sigma. The Bradford protein reagent was from Bio-Rad. DispoEquilibrium dialyzers were obtained from Harvard Apparatus. Ni Sepharose high-performance resin and Ni HisTrap HP columns were from Amersham Biosciences. DNA sequencing was performed by the University of Cincinnati DNA Core. ESI mass spectral analysis (Q-Tof 2; Micromass) was obtained at the University of Cincinnati Mass Spectroscopy Facility. CD spectra were recorded on a JASCO J15 spectrophotometer. 10-Formyl-5,8-dideazafolate (fDDF) and 10-acetyl-5,8-dideazafolate (aDDF) were prepared and quantitated as described previously (*41*, *42*). GAR was prepared by the method of Boschelli et al. (*43*) and purified by anion-exchange chromatography (*40*), and the concentration of the $\beta$-anomer was determined by enzymatic assay with excess fDDF. Recombinant His-tagged TEV protease was produced and purified as described (*44*). The expression vector pTPSN was a generous gift from Prof. Jennifer Doudna.

*Vectors and Bacterial Strains.* The expression vector pMC8HΔT was generated from pMAL-c2x (New England Biolabs). It was digested with *Sac*I and *Ava*I, and this region was replaced with a synthetic oligonucleotide duplex (5′-CGAACCACCACCATCACCACCATCACCACAACC-3′ and 5′-CCGAGGTTGTGGTGATGGTGGTGATGGTG-GTGGTTCGAGCT-3′) that encoded NHHHHHHHHN and complemented the *Sac*I and *Ava*I overhangs. The resulting plasmid, pMAL-c2x-8H, was subjected to site-directed mutagenesis to remove the *Ehe*I site at 1070, without changing the amino acids, to generate pMAL-c2x-8H-Δ. pMAL-c2x-8H-Δ was digested with *Ava*I and *Xmn*I (blunt). The *Ava*−*Xmn* fragment was replaced with a synthetic oligonucleotide duplex prepared from 5′-TCGGGGACT-ACGACATCCCGACCACCGAAAACCTGTACTTCCAG-GGCGCC-3′ and 5′-GGCGCCCTGGAAGTACAGGTTTT-CGTTGTTCGGGATGTCGTAGTCC-3′. This adapter encodes a spacer (GDYDIPTT) and the TEV protease recognition site (ENLYFQ↓G) and contains an *Ava*I overhang and an *Ehe*I site (blunt). The sequences of these vectors were confirmed by dideoxy sequencing. pRARE was isolated from Rosetta(DE3) and used to transform BL21Star(DE3) to generate the expression strain BL21Star(DE3)pRARE. DH5α was used for plasmid production.

*Site-Directed Mutagenesis.* Site-directed mutagenesis was accomplished using the Stratagene QuikChange kit and protocol. The template for mutagenesis was pCC12 (*39*), which contains the coding sequence for the human GAR transformylase (GART) domain in pET17b. Transformed cells were plated on LB agar plates which contained carbenicillin (50 $\mu$g/mL). Small cultures (3 mL) of transformants were grown, and plasmid DNA was isolated using the alkaline lysis method (*45*). The plasmids were screened by restriction digests since the mutagenic primers were designed to introduce or delete restriction sites to facilitate identification of the desired mutants. Positive candidates were sequenced to confirm that only the desired mutation had been introduced.

*Expression Vector Construction.* The coding regions for the wild-type (WT) and mutant GARTs in the pET17b plasmids were amplified using the forward primer 5′-CGTCGTAGTACGAGCGCTCGTGTTGCTGTTCTG-3′ and the reverse primer 5′-CGTACGTACGTGTCGACTCAT-TCCTCTTTAACCC-3′. The forward primer contained an *Eco*47III site while the reverse primer contained a stop codon and a *Sal*I site. The TripleMaster PCR system was employed for these PCR reactions. PCR products were purified,

digested with *Eco*47III and *Sal*I, and ligated with *Ehe*I and *Sal*I digested pMC8HΔT. DH5α cells were transformed with the ligation reactions and plated on LB agar containing carbenicillin (50 μg/mL). Plasmids were isolated from the transformants and screened by digestion with *Ehe*I (successful ligation destroys the unique *Ehe*I site). Positive candidates were confirmed by sequencing. To insert two glycines between the glycine of the TEV protease site and the N-terminal alanine of the GART domain, site-directed mutagenesis was done using the QuikChange kit. The forward primer was 5′-GTACTTCCAGGGCGGTGGCGCCCGTGTTGCTGTTC-3′ and the reverse primer was 5′-GAACAGCAACACGGGCGCCACCGCCCTGGAAGTAC-3′. These contained an *Ehe*I site. Plasmid DNA was isolated and screened by *Ehe*I digestion. Positive candidates were sequenced to confirm the insertion and the integrity of the coding region.

*Protein Production and Purification.* BL21Star(DE3)-pRARE was transformed with pMC8HΔT containing the WT and mutant GART coding regions. Transformed cells were plated on LB agar containing carbenicillin (50 μg/mL) and chloramphenicol (30 μg/mL). A fresh transformant was grown in 500 mL of 2× YT−0.4% glucose−ampicillin (100 μg/mL)−chloramphenicol (30 μg/mL) at 37 °C for ∼22 h. Cells were harvested by centrifugation and resuspended in 500 mL of Terrific broth−ampicillin (100 μg/mL)−chloramphenicol (3 μg/mL). The suspension was shaken at 20 °C for 30 min and induced with IPTG (0.1 mM), and shaking was continued for ∼22 h at 20 °C. Cells were harvested by centrifugation, washed with PBS, and suspended in 50 mL of 20 mM Tris-HCl−250 mM NaCl−2 mM EDTA−10 mM $MgCl_2$, pH 7.5, containing ovomucoid (0.25 mg/mL), SBTI (10 μg/mL), and aprotinin (2.5 μL/mL). The suspension was treated with 100 μL aliquots of the following protease inhibitor solutions: (1) 50 mg/mL benzamidine−1 mg/mL leupeptin ($H_2O$), (2) 1 mg/mL pepstatin (DMSO), and (3) 100 mg/mL PMSF (DMSO). These protease inhibitor solutions were added after each step in the purification. The suspension was treated with lysozyme (10 mg) and DNase (5 units) and incubated on ice for 30 min. Cells were lysed by two passages through a French pressure cell. The lysate was centrifuged at 100000*g* for 1 h. The supernatant was diluted to 100 mL with lysis buffer and brought to 2% streptomycin sulfate by dropwise addition of a 20% aqueous solution over 1 h at 4 °C. This suspension was centrifuged for 20 min at 20000*g*. The supernatant was diluted to 130 mL with PBS and brought to 50% ammonium sulfate saturation by addition of solid (0.291 g/mL) over 30 min, while maintaining the pH at 7.5 with 1 N $NH_4OH$. After 1 h total stirring, the suspension was centrifuged at 20000*g* for 15 min, and the supernatant was dialyzed against 20 mM sodium phosphate, pH 7.4. The dialysate was brought to 10 mM imidazole and 0.5 M NaCl and applied to a 5 mL Ni HisTrap HP column that had been equilibrated with 20 mM sodium phosphate−10 mM imidazole−0.5 M NaCl, pH 7.4. The column was washed with 20 mM sodium phosphate−10 mM imidazole−0.5 M NaCl, pH 7.4 (100 mL), and 20 mM sodium phosphate−25 mM imidazole−0.5 M NaCl, pH 7.4 (50 mL), and eluted with 20 mM sodium phosphate−250 mM imidazole−0.5 M NaCl, pH 7.4. The flow rate was 3 mL/min, and the elution was collected in ∼2.5 mL fractions. Protein-containing fractions ($A_{280}$) were combined and dialyzed against 20 mM Tris-HCl−1 mM EDTA, pH 8.0. The purity of the fusion proteins was assessed by SDS−PAGE.

*Fusion Protein Cleavage.* Digestions were conducted in 50 mM Tris-HCl−1 mM EDTA−1 mM DTT, pH 8.0, for 30 h at room temperature. The molar ratio of fusion protein to TEV protease was 25 to 1. Following digestion, the reaction was dialyzed against 20 mM sodium phosphate−10 mM imidazole−0.5 M NaCl, pH 7.4. The dialysate was applied to a Ni Sepharose high-performance column that had been equilibrated in the same buffer. The amount of resin used was based on a capacity of 40 mg of fusion protein/mL of resin. The flow-through, which contained the desired material, was collected and analyzed by SDS−PAGE. Occasionally the flow-through also contained a small amount of fusion protein. This was removed by precipitation with 50% ammonium sulfate. The ammonium sulfate supernatant was dialyzed against 10 mM potassium phosphate, pH 7.5, and the protein (5−6 mg/mL) was stored in the same buffer containing 10% glycerol at −80 °C.

*Determination of the Extinction Coefficient.* A sample of WT GART was dialyzed against 0.3 M ammonium bicarbonate, pH 7.9, for 48 h. After the UV spectrum was recorded, known volumes of the protein solution were distributed into dried, preweighed microcentrifuge tubes. The samples were lyophilized and stored in a desiccator over $P_2O_5$. Each tube was weighed five times over the course of 3 days. The extinction coefficient was calculated on the basis of the absorbance at 280 nm, the average dry weight, and the calculated molecular weight of the WT GART domain. The value obtained, 16.0 $mM^{-1}$ $cm^{-1}$, was used to quantitate solution concentrations of GART and the mutants since none of the mutations introduced or deleted a chromophore.

*CD Analysis.* CD analysis was performed with a JASCO J15 spectrophotometer at ambient temperature. The molar elipticity was recorded from 195 to 250 nm on protein solutions at 0.1 mg/mL in 10 mM potassium phosphate, pH 7.5.

*Binding Studies.* The dissociation constants for the interaction of WT and mutant GARTs with β-GAR and fDDF were determined in 100 mM Tris-HCl−50 mM NaCl, pH 8.0, using a Harvard Apparatus DispoEquilibrium dialyzer rotating at 8 rpm. An enzyme sample, in the range of 5−65 μM, was dialyzed against a range from 5 to 1000 μM β-GAR or 5−750 μM fDDF for 20 h at 4 °C. Increasing the dialysis time to 30 h did not change the results, indicating that equilibrium had been established in 20 h. The amount of β-GAR or fDDF in each compartment was measured by enzymatic assay with a 10-fold excess of fDDF or β-GAR. To determine the dissociation constant for GAR from the ternary complex, active enzyme was preincubated with aDDF at a concentration equal to 5 times the $K_d$ for fDDF and dialyzed against GAR, and the amount of GAR in each compartment was measured enzymatically with excess fDDF. For inactive enzyme, fDDF, at a concentration equal to 5 times its $K_d$, was used for the preincubation. To determine the dissociation constant for fDDF from the ternary complex, active enzyme was preincubated with GAR-OH (*46*) at a concentration equal to 5 times the $K_d$ for GAR and dialyzed against fDDF, and the amount of fDDF in each compartment was measured enzymatically with excess GAR. For inactive enzyme, GAR, at a concentration equal to 5 times its $K_d$, was used for the preincubation.

*Initial Velocity Studies*. GARTs were assayed in 100 mM Tris-HCl, pH 8.0. The ionic strength was maintained at 0.1 M with NaCl. The assay monitors the formation of 5,8-dideazafolate at 295 nm ($\Delta\epsilon = 18.9$ mM$^{-1}$ cm$^{-1}$) (*42*). The assays were run at 25 °C in a Cary 3E spectrophotometer. Active enzymes were varied from 3 to 6 nM, GAR between 1.25 and 55 $\mu$M, and fDDF between 1.25 and 40 $\mu$M. Inactive mutants (4.5−45 nM) were also assayed with high concentrations (500 $\mu$M) of both substrates. Reactions were initiated with enzyme.

*pH Studies*. The assay was performed, at constant ionic strength, over the pH range 6−10 with saturating concentrations of both substrates. Fixed substrate saturation at each pH was insured by repeating the assays at higher concentrations of the fixed substrate. No change in initial rate was observed upon increasing substrate concentration. The buffer (MTEN) contained 50 mM 2-(*N*-morpholino)ethanesulfonic acid, 25 mM ethanolamine, 25 mM Tris-HCl, and 100 mM NaCl. The stability of the enzymes at the different pHs was assessed by incubating the enzyme at each pH for 15 min at 25 °C and then assaying an aliquot of enzyme in the standard assay (Tris-HCl, pH 8.0) with saturating substrate concentrations.

*Data Processing*. Binding and $k_{cat}$−pH data were fitted to the appropriate equations using a nonlinear least-squares fitting program in KaleidaGraph (version 3.6). Binding data were fitted to eq 1, where [EL] is enzyme−ligand complex concentration, [E] is total enzyme concentration, and [L] is total ligand concentration. $k_{cat}$−pH data were fitted to eq 2, where $y$ is the value of the kinetic parameter, $C$ is the pH-independent value of $y$, $H$ is hydrogen ion concentration, and $K_{a1}$ and $K_{a2}$ are the acid dissociation constants. Initial velocity data were fitted to the equation (eq 3) for a sequential mechanism (*47*) using the Enzyme Kinetics Module 1.1 in SigmaPlot 7. Here, $K_a$ and $K_b$ are the dissociation constants ($K_d$) for the E·GAR and E·fDDF binary complexes, respectively. $\alpha K_a$ and $\alpha K_b$ are the dissociation constants for GAR and fDDF, respectively, from the ternary complex. $\alpha$ is a measure of how the binding of one substrate affects binding of the other substrate (*47*).

$$[EL] = [E][L]/K_d + [L] \quad (1)$$

$$\log y = \log[C/(1 + H/K_{a1} + K_{a2}/H)] \quad (2)$$

$$v = VAB/\alpha K_a K_b + \alpha K_a B + \alpha K_b A + AB \quad (3)$$

## RESULTS

*Enzyme Purification.* Wild-type (*39*) and mutant human GARTs were originally constructed in pET17b. The coding sequences were then transferred into pMC8HΔT as described in Materials and Methods. This generated the enzymes as fusion proteins to the C-terminus of maltose binding protein (MBP). The linker region between the C-terminus of MBP and the N-terminus of GARTs includes an 8-His tag for purification by immobilized metal affinity chromatography (IMAC) (*48*) and a TEV protease cleavage site (*49*) to permit release of GARTs from the fusion partner. A schematic of this construct is shown in Figure 1. The fusion proteins were expressed in BL21Star(DE3)pRARE *E. coli* cells and purified to homogeneity as described in Materials and Methods. The

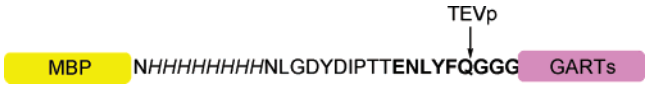


FIGURE 1: Schematic diagram of the MBP fusion protein construct. The bolded section delineates the TEV protease recognition and cleavage sites and includes the three glycines at the N-terminus of the GARTs.

Table 1: Protein Purification Summary for Wild-Type and Mutant GARTs

| protein | fusion protein (mg)[a] | relative yield (%) | enzyme (mg)[b] | relative yield (%) |
|---|---|---|---|---|
| wild type | 330 | 100 | 92 | 100 |
| N106D | 330 | 100 | 58 | 63 |
| N106H | 260 | 79 | 27 | 29 |
| N106Q | 337 | 102 | 78 | 85 |
| H108K | 345 | 105 | 70 | 76 |
| H108R | 260 | 79 | 55 | 60 |
| D144E | 432 | 131 | 98 | 107 |
| D144H | 368 | 112 | 72 | 78 |
| K170R | 300 | 91 | 45 | 49 |

[a] Yield of the purified fusion protein from 500 mL of culture. [b] Yield of the purified cleaved protein.

GARTs were released from their respective fusion proteins by cleavage with TEV protease (*44*). Since the fusion protein and the fusion partner retain the His tag, a second IMAC step served to remove these contaminants, as well as the His-tagged TEV protease, from the GARTs. Occasionally, a small amount of fusion protein was not retained by the second IMAC column. It was removed by precipitation with 50% ammonium sulfate. This procedure afforded all of the GARTs, with three additional glycine residues at the N-terminus, purified to homogeneity in good yield. The insertion of two additional glycines was necessitated by the fact that TEV protease cleavage of the initial fusion proteins was quite inefficient (~50%). The mutants generated, the yields of the fusion proteins, and the yields of the final products are summarized in Table 1. As a measure of global protein integrity, we obtained the CD spectra of wild-type (WT) and mutant GARTs. These were essentially superimposable, indicating that the mutations did not cause gross alterations in protein structure (data not shown).

*Kinetic Parameters and Mechanism.* Initial velocity studies, conducted at the pH maximum for the wild-type enzyme (pH 8.0), afforded the values listed in Table 2. The values for the wild-type enzyme, $k_{cat} = 7.5$ s$^{-1}$, $K_{mGAR} = 1.1 \pm 0.2$ $\mu$M, and $K_{mfDDF} = 0.9 \pm 0.2$ $\mu$M, are comparable to the values obtained previously (*39*) at pH 7.5, $k_{cat} = 6.3$ s$^{-1}$, $K_{mGAR} = 1.1 \pm 0.2$ $\mu$M, and $K_{mfDDF} = 1.5 \pm 0.4$ $\mu$M. The N106Q enzyme has a $k_{cat} = 14$ s$^{-1}$, almost double that of the WT enzyme; however, the $K_m$s for GAR, $29.5 \pm 0.1$ $\mu$M, and fDDF, $19.6 \pm 0.1$ $\mu$M, were increased approximately 27- and 22-fold, respectively. K170R had $k_{cat} = 7.7$ s$^{-1}$, $K_{mGAR} = 1.8 \pm 0.1$ $\mu$M, and $K_{mfDDF} = 1.5 \pm 0.1$ $\mu$M, comparable to the values for the wild-type enzyme. All other mutant enzymes were inactive at pH 8, even with elevated enzyme and substrate concentrations.

The best fits of the initial velocity data were to a random sequential mechanism (eq 3). Our previous (*39*) initial velocity and dead-end inhibition studies on rhGART suggested an ordered sequential mechanism with folate binding first. However, these studies were performed in 0.1 M HEPES buffer. It is likely that HEPES binds to the GAR

Table 2: Steady-State Kinetic Parameters for Wild-Type and Mutant GARTs

| | | | βGAR (μM) | | | fDDF (μM) | | |
|---|---|---|---|---|---|---|---|---|
| enzyme | α | $k_{cat}$ ($s^{-1}$) | $K_d$ | $K_m$[a] | $k_{cat}/K_m$ ($M^{-1}\,s^{-1}$) | $K_d$ | $K_m$[a] | $k_{cat}/K_m$ ($M^{-1}\,s^{-1}$) |
| WT | 0.35 | 7.5 | 3.0 ± 0.7 | 1.1 ± 0.2 | $7.1 \times 10^6$ | 2.6 ± 0.6 | 0.9 ± 0.2 | $8.2 \times 10^6$ |
| N106D | | ND[b] | | | | | | |
| N106H | | ND | | | | | | |
| N106Q | 0.23 | 14.0 | 128.4 ± 0.1 | 29.5 ± 0.1 | $4.7 \times 10^5$ | 85.1 ± 0.1 | 19.6 ± 0.1 | $7.1 \times 10^5$ |
| H108K | | ND | | | | | | |
| H108R | | ND | | | | | | |
| D144E | | ND | | | | | | |
| D144H | | ND | | | | | | |
| K170R | 0.29 | 7.7 | 6.3 ± 0.4 | 1.8 ± 0.1 | $4.3 \times 10^6$ | 5.2 ± 0.4 | 1.5 ± 0.1 | $5.1 \times 10^6$ |

[a] $\alpha K_d$. [b] No activity detected.

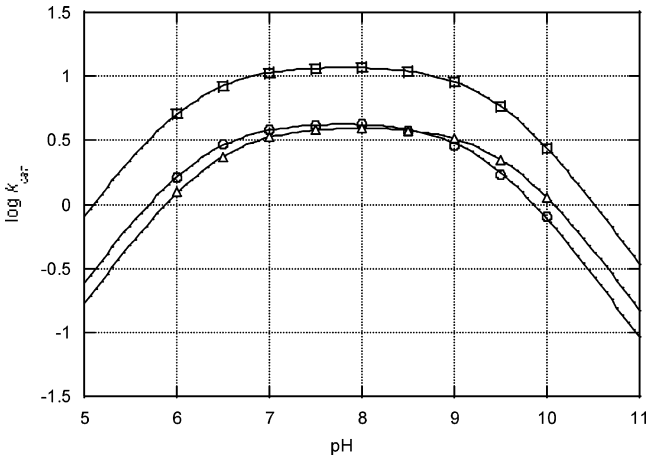


FIGURE 2: pH−rate profiles for the WT (○), N106Q (□), and K170R (△) enzymes.

phosphate site, effectively acting as a competitve inhibitor and thus skewing the kinetic patterns.

*pH−Rate Profiles.* The $k_{cat}$ versus pH data for WT, N106Q, and K170R GARTs are shown in Figure 2. These data show bell-shaped curves with limiting slopes of 1 and pH maximums of 8. Fitting of the data to eq 2 yielded two p$K_a$ values of 6.23 ± 0.02 and 9.32 ± 0.02 for the WT enzyme, 6.15 ± 0.005 and 9.46 ± 0.003 for the N106Q mutant, and 6.37 ± 0.006 and 9.57 ± 0.006 for the K170R mutant. All three proteins were stable over the entire pH range as determined by incubation for 15 min at each pH, followed by assaying of an aliquot of the protein at pH 8 with saturating concentrations of both substrates. The $k_{cat}$s for all three active enzymes in MTEN at pH 8 were lower than those obtained in the standard assay at pH 8. The $k_{cat}$s for WT (4.5 $s^{-1}$), N106Q (12.2 $s^{-1}$), and K170R (4.1 $s^{-1}$) were 60%, 87%, and 53%, respectively, of those obtained in Tris-HCl at pH 8 and comparable ionic strength.

*Substrate Binding: Binary Complexes.* Equilibrium dialysis was employed to determine the dissociation constants for β-GAR and fDDF for the WT and the mutant enzymes. These data are summarized in Table 3. For the WT enzyme, the dissociation constants for GAR and fDDF, 3.0 ± 0.2 and 2.8 ± 0.2 μM, respectively, are the same as what were determined from the initial velocity studies (Table 2). The $K_d$ for β-GAR for the active N106Q mutant, 73.5 ± 2.2 μM, was about 40% lower than that obtained from the initial velocity studies, 128.4 ± 0.1 μM, but the $K_d$s for fDDF were essentially the same, 84.2 ± 2.4 μM (equilibrium dialysis) vs 85.1 ± 0.1 μM (Table 2). The active K170R mutant had a $K_d$ for GAR of 6.1 ± 0.1 μM and a $K_d$ for fDDF of 6.5 ± 0.1 μM. These are very close to the values of 6.3 ± 0.4 and 5.2 ± 0.4 μM obtained from the initial velocity studies (Table 2).

We were unable to detect any binding of GAR to the inactive mutants H108K, H108R, D144E, and D144H; however, these mutants were able to bind fDDF with $K_d$s of 82.1 ± 3.3, 63.1 ± 1.1, 126.1 ± 5.8, and 67.0 ± 0.1 μM, respectively. In contrast, the inactive N106D and N106H mutants were able to bind both GAR and fDDF, with $K_d$s of 65.8 ± 2.6 and 152.5 ± 4.4 μM for GAR, respectively, and $K_d$s of 23.5 ± 0.5 and 58.1 ± 1.2 μM for fDDF, respectively.

*Substrate Binding: Ternary Complexes.* Equilibrium dialysis was also employed to determine the dissociation constants of each of the substrates from the ternary complex. The competitive inhibitors GAR-OH (*46*) and aDDF (*41*) were used in place of GAR and fDDF, respectively, with the active enzymes. These data are included in Table 3. For the WT enzyme, the presence of the second substrate analogue did not alter either of the $K_d$s. For the active N106Q and K170R mutants, the $K_d$s for GAR were essentially unaffected by saturating aDDF. We were unable to determine the $K_d$s for fDDF of the active mutants in the presence of GAR-OH because, at the high concentration of enzyme (20 μM) and GAR-OH (360 μM) required, there was turnover of fDDF (*28*).

The inactive mutants that did not form a binary complex with GAR, H108K, H108R, D144E, and D144H, were able to form the ternary complex in the presence of saturating fDDF, with $K_d$s for GAR of 109.8 ± 11.0, 84.0 ± 1.2, 35.4 ± 1.1, and 75.3 ± 2.6 μM, respectively (Table 3). In addition, the binding of fDDF by these proteins was affected by the presence of GAR. For H108K and D144E, the $K_d$s for fDDF of 60.6 ± 1.2 and 48.5 ± 0.2 μM were lower than in the absence of GAR, 82.1 ± 3.2 and 126.1 ± 5.8 μM. In contrast, the $K_d$s of H108R and D144H for fDDF, 97.9 ± 1.7 and 80.0 ± 2.1 μM, in the presence of GAR were higher than in its absence, 63.1 ± 1.1 and 67.0 ± 0.1 μM (Table 3).

## DISCUSSION

Our initial targets for site-directed mutagenesis were N106, H108, D144, and K170. The first three are wholly conserved in all GARTs examined to date, while K170 is conserved in the chicken and mouse enzymes, replaced by Q in the *E. coli* enzyme, and replaced by H in the *Drosophila melanogaster*, *Bacillus subtilis*, and *Saccharomyces cerevisiae* enzymes (*25*). N106, H108, and D144 were chosen here

Table 3: Substrate Binding Data for GART and Mutants

| | β-GAR[a] | | β-GAR[b] | | fDDF[c] | | fDDF[d] | |
|---|---|---|---|---|---|---|---|---|
| enzyme | $K_d$ (μM) | $\Delta G$[e] | $K_d$ (μM) | $\Delta G$ | $K_d$ (μM) | $\Delta G$ | $K_d$ (μM) | $\Delta G$ |
| WT | 3.0 ± 0.2 | 7.5 | 3.1 ± 0.3 | 7.5 | 2.8 ± 0.2 | 7.6 | 2.9 ± 0.1 | 7.6 |
| N106D | 65.8 ± 2.6 | 5.7 | 56.8 ± 1.2 | 5.8 | 23.5 ± 0.5 | 6.3 | 11.2 ± 0.2 | 6.7 |
| N106H | 152.5 ± 4.4 | 5.2 | 43.6 ± 0.8 | 5.9 | 58.1 ± 1.2 | 5.8 | 29.8 ± 1.2 | 6.1 |
| N106Q | 73.5 ± 2.2 | 5.6 | 75.2 ± 3.2 | 5.6 | 84.2 ± 2.4 | 5.5 | NO[f] | |
| H108K | ND[g] | | 109.8 ± 11.0 | 5.4 | 82.1 ± 3.2 | 5.6 | 60.6 ± 1.2 | 5.7 |
| H108R | ND | | 84.0 ± 1.2 | 5.5 | 63.1 ± 1.1 | 5.7 | 97.9 ± 1.7 | 5.4 |
| D144E | ND | | 35.4 ± 1.1 | 6.0 | 126.1 ± 5.8 | 5.3 | 48.5 ± 0.2 | 5.9 |
| D144H | ND | | 75.3 ± 2.6 | 5.6 | 67.0 ± 0.1 | 5.7 | 80.0 ± 2.1 | 5.6 |
| K170R | 6.1 ± 0.1 | 7.1 | 8.1 ± 0.2 | 6.9 | 6.5 ± 0.1 | 7.0 | NO | |

[a] Determined in the absence of fDDF or aDDF. [b] Determined in the presence of fDDF or aDDF. [c] Determined in the absence of GAR or GAR-OH. [d] Determined in the presence of GAR or GAR-OH. [e] Calculated from the equation $\Delta G = -RT \ln K_d$. Values are in kcal/mol. [f] Not obtainable. [g] None detected.

because they have been implicated in the mechanism of action of both the *E. coli* and human enzymes.

N106 is proposed to stabilize the oxyanion in the putative tetrahedral intermediate (Scheme 1), while D144 is suggested to form a salt bridge to protonated H108 which, in turn, forms a hydrogen bond to the formyl carbonyl oxygen, increasing the electrophilicity of the formyl carbonyl carbon (*14*). In *E. coli* GART, Q170 forms hydrogen bonds to both the GAR phosphate oxygen and the 3′-hydroxyl (*11*), while in human GART, K170 appears to interact only with the GAR phosphate oxygen (*27*). These observations have implications for GAR binding. It is expected that the positively charged ϵ-ammonium of K170 will interact electrostatically with the phosphate oxygen, resulting in a tighter association than that afforded with Q170 (*E. coli*). Indeed, rhGART has a $K_m$ for GAR, 1.1 ± 0.2 μM (Table 2), that is approximately 100-fold lower than that of *E. coli* GART, 118 ± 3 μM (*8*).

The substitutions chosen and the rationale for each follow. N106 was substituted with D, H, and Q. If the proposed role for N106 is correct, then the presumed negative charge of the N106D substitution should destabilize the oxyanion in the tetrahedral intermediate, leading to a diminished $k_{cat}$ if formation of the tetrahedral intermediate is wholly or partially rate limiting or an increased $k_{cat}$ if the collapse of the intermediate is partially or wholly rate limiting. Indeed, no activity was observed for this mutant, tentatively suggesting that formation of the tetrahedral intermediate is, at least partially, rate limiting since the N to D substitution should not impose any steric constraints. In contrast, the N106D mutant of the *E. coli* enzyme did show some activity (*6*).

N106H also tests mechanistic proposals. If H is protonated, this change should lead to an increase in $k_{cat}$ due to proton donation to the formyl carbonyl oxygen or to the departing amine. A decrease in $k_{cat}$ would be expected if H is not protonated or if this substitution is sterically unacceptable. This substitution resulted in inactive enzyme, but additional information is needed before a definitive mechanistic conclusion can be drawn. N106H *E. coli* GART was also inactive (*6*).

N106Q is a conservative replacement meant to test steric constraints within the enzyme active site. N106Q is catalytically active with a $k_{cat}$ almost 2-fold higher than the WT enzyme, although the $K_m$s for both substrates are increased approximately 25-fold (Table 2), indicating that the N to Q substitution is sterically acceptable. Interestingly, N106Q was not obtained in a saturation site-directed mutagenesis study of *E. coli* GART (*6*).

H108 was converted to K and R. As noted above, H108 is proposed to be protonated ($pK_a = 9.7$) (*9*) and in a salt bridge with D144. Protonated H108 then acts as a general acid catalyst to accelerate formation of the tetrahedral intermediate. If steric constraints are not an issue, the K and R, with their higher $pK_a$s, should be better general acid catalysts, and these substitutions are predicted to increase $k_{cat}$. However, if neutral H108 is required to facilitate collapse of the tetrahedral intermediate to products, then K and R would be unacceptable since they would remain protonated over the relevant pH range. Neither of these mutant proteins were active, suggesting that neutral H108, acting as a general base, is required for product formation, in the absence of steric issues with these substitutions. In the saturation site-directed mutagenesis study of *E. coli* GART (*6*), H108R was inactive, while H108K was not obtained.

Ionized D144 is proposed to form a salt bridge with protonated H108, and this "catalytic dyad" then provides general acid catalysis for formation of the tetrahedral intermediate. D144E, a conservative replacement, was inactive. D114H was also inactive. Whether H is neutral or protonated, the putative salt bridge between D144 and H108 would be disrupted, leading to diminished or obliterated catalytic activity. Although D144H *E. coli* GART was inactive, the D144E mutant was active, albeit much less active than the WT enzyme (*6*).

As noted above, K170 is not wholly conserved, but it participates in electrostatic interactions with the GAR phosphate group in rhGART (and presumably in chicken and mouse GARTs). The conservative replacement of K by R results in an enzyme with kinetic parameters almost identical to those of the WT enzyme (Table 2), as would be predicted.

For the inactive mutants the question arises as to whether the inactivity results from affecting a catalytically essential residue or simply from destroying the enzyme's ability to bind its substrates. Gross structural alterations caused by the mutations were ruled out by the CD data. We employed equilibrium dialysis to assess binary and ternary complex formation for WT and all of the mutant proteins, and these data are collected in Table 3. All of the inactive mutants were able to form the binary complex with fDDF and, more importantly, the ternary complex, thus ruling out impaired substrate binding as the source of catalytic inactivity. Four of the inactive mutants, H108K, H108R, D144E, and D144H, were unable to bind GAR in the absence of fDDF. A reasonable conclusion is that, for these four mutants, folate binding is required to "order" the folate binding loop

(residues 141−146) to prepare the active site for substrate, GAR, binding. We hope to obtain structural evidence to address this question. Controversy surrounds this loop in the native enzyme. In the structure of "apo" rhGART at pH 8.5 (enzyme active), that contains phosphate in the GAR site, the loop is flexible and becomes ordered when a folate analogue binds (*27*). In contrast, our apo (unoccupied GAR site) and ternary complex structures at pH 6.3 (enzyme active) showed essentially identical, ordered structures for this loop. Our binding studies with the WT enzyme conducted at pH 8, the pH for maximum activity, showed independent binding for GAR and fDDF, suggesting that folate binding is not a prerequisite for organizing the active site for productive substrate binding and catalysis, which is consistent with our (see above) and other kinetic studies (*8*, *50*) which yielded a random sequential kinetic mechanism.

pH−rate profiles were generated for the WT enzyme and the active mutants, N106Q and K170R. These all gave rate maxima at pH 8, as seen previously for rhGART (*27*), and p$K_a$s and bell-shaped curves (Figure 2) similar to what were obtained for *E. coli* GART (*9*). These results lead us to conclude that the ionizations in the rhGART ternary complex involve the same groups as proposed for *E. coli* GART, namely, protonation of the amino group of GAR on the acid leg and deprotonation of H108 on the base leg, both of which lead to loss of enzymatic activity. Earlier studies from this laboratory (*51*) suggested that GAR, as the unprotonated amine, is the active substrate species. We used the same buffer (MTEN) as was used in the *E. coli* study to facilitate direct comparison. However, the human enzymes displayed reduced activity in this buffer. This is probably due to the 2-(*N*-morpholino)ethanesulfonate binding to the GAR phosphate site, acting as a competitive inhibitor, and reflects the higher affinity of the human vs *E. coli* enzyme for the GAR phosphate moiety (see above).

## CONCLUSIONS

Site-directed mutagenesis of putative catalytic residues in human GART supports the proposal that N106, H108, and D144 are essential for catalytic activity. This conclusion is further bolstered by the substrate binding studies, which clearly indicate that loss of catalytic activity for the inactive mutants is not due to their inability to bind substrates, and the pH−rate profiles. The steady-state kinetics of the WT, N106Q, and K170R enzymes indicated a random sequential kinetic mechanism, consistent with the kinetic behavior of the *E. coli* (*8*) and mouse (*50*) enzymes. The kinetic mechanism is reinforced by results from the binding studies which showed independent binding of GAR and fDDF. Finally, these studies again provide evidence of differences between *E. coli* and human GART.

## ACKNOWLEDGMENT

We thank Dr. Apryll Stalcup, Department of Chemistry, University of Cincinnati, for allowing us to use her CD spectrophotometer.

## REFERENCES

1. Warren, L., and Buchanan, J. M. (1957) Biosynthesis of the purines. XIX. 2-Amino-N-ribosylacetamide 5′-phosphate (glycinamide ribotide) transformylase, *J. Biol. Chem. 229*, 613−626.
2. Divekar, A. Y., and Hakala, M. T. (1975) Inhibition of the biosynthesis of 5′-phosphoribosyl-N-formylglycinamide in sarcoma 180 cells by homofolate, *Mol. Pharmacol. 11*, 319−325.
3. Moran, R. G. (1991) Folate antimetabolites inhibitory to *de novo* purine synthesis, *Cancer Treat. Res. 58*, 65−87.
4. Berman, E. M., and Werbel, L. M. (1991) The renewed potential for folate antagonists in contemporary cancer chemotherapy, *J. Med. Chem. 34*, 479−485.
5. Beardsley, G. P., Moroson, B. A., Taylor, E. C., and Moran, R. G. (1989) A new folate antimetabolite, 5,10-dideaza-5,6,7,8-tetrahydrofolate is a potent inhibitor of *de novo* purine synthesis, *J. Biol. Chem. 264*, 328−333.
6. Warren, M. S., and Benkovic, S. J. (1996) A rapid screen of active site mutants in glycinamide ribonucleotide transformylase, *Biochemistry 35*, 8855−8862.
7. Warren, M. S., and Benkovic, S. J. (1997) Combinatorial manipulation of three key active site residues in glycinamide ribonucleotide transformylase, *Protein Eng. 10*, 63−68.
8. Shim, J. H., and Benkovic, S. J. (1998) Evaluation of the kinetic mechanism of *Escherichia coli* glycinamide ribonucleotide transformylase, *Biochemistry 37*, 8776−8782.
9. Shim, J. H., and Benkovic, S. J. (1999) Catalytic mechanism of *Escherichia coli* glycinamide ribonucleotide transformylase probed by site-directed mutagenesis and pH-dependent studies, *Biochemistry 38*, 10024−10031.
10. Su, Y., Yamashita, M. M., Greasley, S. E., Mullen, C. A., Shim, J. H., Jennings, P. A., Benkovic, S. J., and Wilson, I. A. (1998) A pH-dependent stabilization of an active site loop observed from low and high pH crystal structures of mutant monomeric glycinamide ribonucleotide transformylase at 1.8 to 1.9 Å, *J. Mol. Biol. 281*, 485−499.
11. Almassy, R. J., Janson, C. A., Kan, C.-C., and Hostomska, K. (1992) Structures of *apo* and complexed *Escherichia coli* glycinamide ribonucleotide transformylase, *Proc. Natl. Acad. Sci. U.S.A. 89*, 6114−6118.
12. Chen, P., Schulze-Gahmen, U., Stura, E. A., Inglese, J., Johnson, D. L., Marolewski, A., Benkovic, S. J., and Wilson, I. A. (1992) Crystal structure of glycinamide ribonucleotide transformylase from *Escherichia coli* at 3.0 Å resolution. A target enzyme for chemotherapy, *J. Mol. Biol. 227*, 283−292.
13. Greasley, S. E., Yamashita, M. M., Cai, H., Benkovic, S. J., Boger, D. L., and Wilson, I. A. (1999) New insights into inhibitor design from the crystal structure and NMR studies of *Escherichia coli* GAR transformylase in complex with $\beta$-GAR and 10-formyl-5,8,10-trideazafolic acid, *Biochemistry 38*, 16783−16793.
14. Klein, C., Chen, P., Arevalo, J. H., Stura, E. A., Marolewski, A., Warren, M. S., Benkovic, S. J., and Wilson, I. A. (1995) Towards structure-based drug design: crystal structure of a multisubstrate adduct complex of glycinamide ribonucleotide transformylase at 1.96 Å resolution, *J. Mol. Biol. 249*, 153−175.
15. Greasley, S. E., Marsilje, T. H., Cai, H., Baker, S., Benkovic, S. J., Boger, D. L., and Wilson, I. A. (2001) Unexpected formation of an epoxide-derived multisubstrate adduct inhibitor on the active site of GAR transformylase, *Biochemistry 40*, 13538−13547.
16. Boger, D. L., Haynes, N.-E., Kitos, P. A., Warren, M. S., Ramcharan, J., Marolewski, A. E., and Benkovic, S. J. (1997) 10-Formyl-5,8,10-trideazafolic acid (10-formyl-TDAF): a potent inhibitor of glycinamide ribonucleotide transformylase, *Bioorg. Med. Chem. 5*, 1817−1830.
17. Boger, D. L., Haynes, N.-E., Warren, M. S., Gooljarsingh, L. T., Ramcharan, J., Kitos, P. A., and Benkovic, S. J. (1997) Functionalized analogues of 5,8,10-trideazafolate as potential inhibitors of GAR Tfase or AICAR Tfase, *Bioorg. Med. Chem. 5*, 1831−1838.
18. Boger, D. L., Haynes, N.-E., Warren, M. S., Ramcharan, J., Kitos, P. A., and Benkovic, S. J. (1997) Functionalized analogues of 5,8,10-trideazafolate: development of an enzyme-assembled tight binding inhibitor of GAR Tfase and a potential irreversible inhibitor of AICAR Tfase, *Bioorg. Med. Chem. 5*, 1839−1846.
19. Boger, D. L., Haynes, N.-E., Warren, M. S., Ramcharan, J., Marolewski, A. E., Kitos, P. A., and Benkovic, S. J. (1997) Abenzyl 10-formyl-trideazafolic acid (abenzyl 10-formyl-TDAF): an effective inhibitor of glycinamide ribonucleotide transformylase, *Bioorg. Med. Chem. 5*, 1847−1852.
20. Boger, D. L., Haynes, N.-E., Warren, M. S., Ramcharan, J.,Kitos, P. A., and Benkovic, S. J. (1997) Multisubstrate analogue based on 5,8,10-trideazafolate, *Bioorg. Med. Chem. 5*, 1853−1857.
21. Boger, D. L., Kochanny, M. J., Cai, H., Wyatt, D., Kitos, P. A., Warren, M. S., Ramcharan, J., Gooljarsingh, L. T., and Benkovic,

S. J. (1998) Design, synthesis, and evaluation of potential GAR and AICAR transformylase inhibitors, *Bioorg. Med. Chem. 6*, 643−659.
22. Boger, D. L., Labroli, M. A., Marsilje, T. H., Jin, Q., Hedrick, M. P., Baker, S. J., Shim, J. H., and Benkovic, S. J. (2000) Conformationally restricted analogues designed for selective inhibition of GAR Tfase versus thymidylate synthase or dihydrofolate reductase, *Bioorg. Med. Chem. 8*, 1075−1086.
23. Smith, J. M., and Daum, H. A., III (1987) Identification and nucleotide sequence of a gene encoding 5′-phosphoribosylglycinamide transformylase in *Escherichia coli* K12, *J. Biol. Chem. 262*, 10565−10569.
24. Inglese, J., Johnson, D. L., Shiau, A., Smith, J. M., and Benkovic, S. J. (1990) Subcloning, characterization, and affinity labeling of *Escherichia coli* glycinamide ribonucleotide transformylase, *Biochemistry 29*, 1436−1443.
25. Aimi, J., Qiu, H., Williams, J., Zalkin, H., and Dixon, J. E. (1990) *De novo* purine nucleotide biosynthesis: cloning of human and avian cDNAs encoding the trifunctional glycinamide ribonucleotide synthetase-aminoimidazole ribonucleotide synthetase-glycinamide ribonucleotide transformylase by functional complementation in *E. coli*, *Nucleic Acids Res. 18*, 6665−6672.
26. Schild, D., Brake, A. J., Kiefer, M. C., Young, D., and Barr, P. J. (1990) Cloning of three human multifunctional *de novo* purine biosynthetic genes by functional complementation of yeast mutations, *Proc. Natl. Acad. Sci. U.S.A. 87*, 2916−2920.
27. Zhang, Y., Desharnais, J., Greasley, S. E., Beardsley, G. P., Boger, D. L., and Wison, I. A. (2002) Crystal structure of human GAR Tfase at low and high pH and with substrate $\beta$-GAR, *Biochemistry 41*, 14206−14215.
28. Dahms, T. E., Sainz, G., Giroux, E. L., Caperelli, C. A., and Smith, J. L. (2005) The *apo* and ternary complex structures of a chemotherapeutic target: human glycinamide ribonucleotide transformylase, *Biochemistry 44*, 9841−9850.
29. Varney, M. D., Palmer, C. L., Romines, W. H., III, Boritzki, T., Margosiak, S. A., Almassy, R., Janson, C. A., Bartlett, C., Howland, E. J., and Ferre, R. (1997) Protein sturcture-based design, synthesis, and biological evaluation of 5-thia-2,6-diamino-4(3*H*)-oxopyrimidines: potent inhibitors of glycinamide ribonucleotide transformylase with potent cell growth inhibition, *J. Med. Chem. 40*, 2502−2524.
30. Marsilje, T. H., Labroli, M. A., Hedrick, M. P., Jin, Q., Desharnais, J., Baker, S. J., Gooljarsingh, L. T., Ramcharan, J., Tavassoli, A., Zhang, Y., Wilson, I. A., Beardsley, G. P., Benkovic, S. J., and Boger, D. L. (2002) 10-Formyl-5,10-dideaza-acyclic-5,6,7,8-tetrahydrofolic acid (10-formyl-DDACTHF): a potent cytotoxic agent acting by selective inhibition of human GAR Tfase and the *de novo* purine biosynthetic pathway, *Bioorg. Med. Chem. 10*, 2739−2749.
31. Zhang, Y., Desharnais, J., Marsilje, T. H., Li, C., Hedrick, M. P., Gooljarsingh, L. T., Tavassoli, A., Benkovic, S. J., Olson, A. J., Boger, D. L., and Wilson, I. A. (2003) Rational design, synthesis, evaluation, and crystal structure of a potent inhibitor of human GAR Tfase: 10-(trifluoroacetyl)-5,10-dideazaacyclic-5,6,7,8-tetrahydrofolic acid, *Biochemistry 42*, 6043−6056.
32. Marsilje, T. H., Hedrick, M. P., Desharnais, J., Tavassoli, A., Zhang, Y., Wilson, I. A., Benkovic, S. J., and Boger, D. L. (2003) Design, synthesis, and biological evaluation of simplified $\alpha$-keto heterocycle, trifluoromethyl ketone, and formyl substituted folate analogues as potential inhibitors of GAR transformylase and AICAR transformylase, *Bioorg. Med. Chem. 11*, 4487−4501.
33. Marsilje, T. H., Hedrick, M. P., Desharnais, J., Capps, K., Tavassoli, A., Zhang, Y., Wilson, I. A., Benkovic, S. J., and Boger, D. L. (2003) 10-(2-benzoxazolcarbonyl)-5,10-dideaza-acyclic-5,6,7,8-tetrahydrofolic acid: a potential inhibitor of GAR transformylase and AICAR transformylase, *Bioorg. Med. Chem. 11*, 4503−4509.
34. Desharnais, J., Hwang, I., Zhang, Y., Tavassoli, A., Baboval, J., Benkovic, S. J., Wilson, I. A., and Boger, D. L. (2003) Design, synthesis and biological evaluation of 10-$CF_3$CO-DDACTHF analogues and derivatives as inhibitors of GAR Tfase and the *de novo* purine biosynthetic pathway, *Bioorg. Med. Chem. 11*, 4511−4521.
35. Cheng, H., Chong, I., Hwang, I., Tavassoli, A., Zhang, Y., Wilson, I. A., Benkovic, S. J., and Boger, D. L. (2005) Design, synthesis and biological evaluation of 10-methanesulfonyl-DDACTHF, 10-methanesulfonyl-5-DACTHF, and 10-methylthio- DDACTHF as potent inhibitors of GAR Tfase and the *de novo* purine biosynthetic pathway, *Bioorg. Med. Chem. 13*, 3577−3585.
36. Chong, Y., Hwang, I., Tavassoli, A., Zhang, Y., Wilson, I. A., Benkovic, S. J., and Boger, D. L. (2005) Synthesis and biological evaluation of $\alpha$- and -$\gamma$-carboxamide derivatives of 10-$CF_3$CO-DDACTHF, *Bioorg. Med. Chem. 13*, 3587−3592.
37. Cheng, H., Hwang, I., Chong, Y., Tavassoli, A., Webb, M. E., Zhang, Y., Wilson, I. A., Benkovic, S. J., and Boger, D. L. (2005) Synthesis and biological evaluation of N-{4-[5-(2,4-diamino-6-oxo-1,6-dihydropyrimidin-5-yl)-2-(2,2,2-trifluoroacetyl)pentyl]-benzoyl}-L-glutamic acid as a potential inhibitor of GAR Tfase and the *de novo* purine biosynthetic pathway, *Bioorg. Med. Chem. 13*, 3593−3599.
38. Kan, C.-C., Gehring, M. R., Nodes, B. R., Janson, C. A., Almassy, R. J., and Hostomska, Z. (1992) Heterologous expression and purification of active human phosphoribosylglycinamide formyltransferase as a single domain, *J. Protein Chem. 11*, 467−473.
39. Caperelli, C. A., and Giroux, E. L. (1997) The human glycinamide ribonucleotide transformylase domain: purification, characterization, and kinetic mechanism, *Arch. Biochem. Biophys. 341*, 98−103.
40. Antle, V. D., Donat, N., Hua, M., Liao, P.-L., Vince, R., and Caperelli, C. A. (1999) Substrate specificity of human glycinamide ribonucleotide transformylase, *Arch. Biochem. Biophys. 370*, 231−235.
41. Caperelli, C. A., and Conigliaro, J. (1986) Synthesis of 10-acetyl-5,8-dideazafolic acid: a potent inhibitor of glycinamide ribonucleotide transformylase, *J. Med. Chem. 29*, 2117−2119.
42. Smith, G. K., Mueller, W. T., Benkovic, P. A., and Benkovic, S. J. (1981) On the cofactor specificity of glycinamide ribonucleotide and 5-aminoimidazole-4-carboxamide ribonucleotide transformylase from chicken liver, *Biochemistry 20*, 1241−1245.
43. Boschelli, D. H., Powell, D., Sharky, V., and Semmelhack, M. F. (1989) An improved synthesis of glycinamide ribonucleotide, *Tetrahedron Lett. 30*, 1599−1600.
44. Lucast, L. J., Batey, R. T., and Doudna, J. A. (2001) Large-scale purification of a stable form of recombinant tobacco etch virus protease, *BioTechniques 30*, 544−554.
45. Birnboim, H. C., and Doly, J. (1979) A rapid alkaline extraction procedure for screening recombinant plasmid DNA, *Nucleic Acids Res. 7*, 1513−1523.
46. Schendel, F. J., and Stubbe, J. (1986) Substrate specificity of formylglycinamidine synthetase, *Biochemistry 25*, 2256−2264.
47. Segel, I. H. (1975) *Enzyme Kinetics: Behavior and Analysis of Rapid Equilibrium and Steady-State Enzyme Systems*, pp 274−291, Wiley-Interscience, New York.
48. Porath, J., Carlsson, J., Olsson, I., and Belfrage, G. (1975) Metal chelate affinity chromatography, a new approach to protein fractionation, *Nature 258*, 598−599.
49. Dougherty, W. G., Carrington, J. C., Cary, S. M., and Parks, T. D. (1988) Biochemical and mutational analysis of a plant virus polyprotein cleavage site, *EMBO J. 7*, 1281−1287.
50. Sanghani, S. P., and Moran, R. G. (1997) Tight binding of folate substrates and inhibitors to recombinant mouse glycinamide ribonucleotide formyltransferase, *Biochemistry 36*, 10506−10516.
51. Caperelli, C. A. (1989) Mammalian glycinamide ribonucleotide transformylase: Kinetic mechanism and associated *de novo* purine biosynthetic activities, *J. Biol. Chem. 264*, 5053−5057.

BI0619270